

NASA Technical Memorandum 103625
AIAA-90-3932

The Effect of Swirl Recovery Vanes on the Cruise Noise of an Advanced Propeller

James H. Dittmar
National Aeronautics and Space Administration
Lewis Research Center
Cleveland, Ohio

and

David G. Hall
Sverdrup Technology, Inc.
Lewis Research Center Group
Brook Park, Ohio

Prepared for the
13th Aeroacoustics Conference
sponsored by the American Institute of Aeronautics and Astronautics
Tallahassee, Florida, October 22-24, 1990



(NASA-TP-103625) THE EFFECT OF SWIRL
RECOVERY VANES ON THE CRUISE NOISE OF AN
ADVANCED PROPELLER (NASA) 103625-1 CSCL 20A

NR1-11494

Unclass

01/77 011149

THE EFFECT OF SWIRL RECOVERY VANES ON THE CRUISE NOISE OF AN ADVANCED PROPELLER

James H. Dittmar
National Aeronautics and Space Administration
Lewis Research Center
Cleveland, Ohio 44135

and

David G. Hall
Sverdrup Technology, Inc.
Lewis Research Center Group
Brook Park, Ohio 44142

SUMMARY

The SR-7A propeller was acoustically tested with and without downstream swirl recovery vanes to determine if any extra noise was caused by the interaction of the propeller wakes and vortices with these vanes. No additional noise was observed at the cruise condition over the angular range tested. The presence of the swirl recovery vanes did unload the propeller and some small peak noise reductions were observed from lower propeller loading noise. The propeller was also tested alone to investigate the behavior of the peak propeller noise with helical tip Mach number. As observed before on other propellers, the peak noise first rose with helical tip Mach number and then leveled off or decreased at higher helical tip Mach numbers. Detailed pressure-time histories indicate that a portion of the primary pressure pulse is progressively cancelled by a secondary pulse as the helical tip Mach number is increased. This cancellation appears to be responsible for the peak noise behavior at high helical tip Mach numbers.

INTRODUCTION

Advanced turboprop-powered aircraft have the potential for significant fuel savings over equivalent core technology turbofan-powered aircraft. To investigate this potential, NASA has an ongoing Advanced Turboprop Program. Both single and counterrotation propellers have been investigated by NASA. Counterrotation propellers have a theoretically higher efficiency than single rotation propellers because the second row of blades is able to recover some of the residual swirl left from the forward set of blades. In this investigation, a single rotation model propeller was tested with and without a fixed set of swirl recovery vanes behind the propeller. The intent of these vanes is to recover some of the residual swirl from the propeller without the added complication of a second set of rotating blades as exists in the counterrotation propeller. A photograph of this single rotation model with swirl recovery vanes is shown in figure 1(a).

The noise generated by advanced propellers is of concern as a cabin environment problem for the airplane at cruise. Cruise noise measurements of single rotation propeller models (refs. 1 to 4) and counterrotation propeller models (refs. 5 to 7) have been made previously in the NASA Lewis Research Center 8- by 6-Foot Wind Tunnel. Counterrotation propellers show an additional

cruise noise component over single rotation propellers caused by the interaction of the upstream blade wakes and vortices with the downstream blades. Figure 2 (from ref. 5) shows the cruise noise directivity of a counterrotation propeller. The tone noise at twice blade passing frequency is plotted here showing propeller alone and interaction components. The propeller alone tones from the two rotors are seen to dominate the noise near the peak, but the interaction component is seen to make a contribution to the total noise at the far forward and far aft positions. The interaction noise could be separated from the propeller alone tones for this counterrotation propeller because the interaction tone occurs at a different frequency. Since the swirl recovery vanes also intercept the propeller wakes and vortices, interaction noise can be generated here also. Noise measurements were made for a single rotation propeller with and without these swirl recovery vanes to assess the amount of interaction noise that might be generated. Here, since the vanes do not rotate, the interaction noise is radiated at the propeller blade passing tone and its harmonics. As a result, this interaction noise is not separable as for the counterrotation case and would only be seen as an increase in the total noise at each harmonic. This report presents the results of acoustic measurements taken in the NASA 8- by 6-Foot Wind Tunnel at cruise conditions for the SR-7A propeller with and without swirl recovery vanes.

APPARATUS AND PROCEDURE

Swirl Recovery Vanes

An eight bladed single rotation propeller, designated SR-7A, was tested with and without swirl recovery vanes. Figure 1(a) is a photograph of these vanes behind the SR-7A propeller model. An individual blade is shown in figure 1(b) and a swirl recovery vane is shown in figure 1(c). This model had eight swirl recovery vanes with a leading edge hub-to-tip sweep of approximately 45° . The swirl recovery vanes were tested in two axial positions as illustrated in figure 3. The propeller was tested at three blade setting angles, 63.3° , 60.2° , and 57.7° , with the swirl recovery vane setting angle set at 86.1° . This was done at both forward and aft spacings for tunnel Mach numbers varying from 0.6 to 0.8. At the forward spacing the propeller was also tested at the 63.3° blade setting angle with the vanes set at 87.5° and 84.7° . The propeller was also tested by itself without the swirl recovery vanes at the nominal blade setting angles of 63.3° , 60.2° , and 57.7° . In addition, the propeller was tested alone at the 60.2° blade setting angle at an advance ratio of 3.06 for tunnel Mach numbers of 0.6 to 0.86 to obtain propeller pressure-time histories.

Acoustic Measurements

A plate was mounted from the tunnel ceiling, 0.3 propeller diameters from the tip, and transducers were installed flush with the plate surface to measure the noise. A photograph of this plate is shown in figure 4(a) and a sketch of the installed plate is shown in figure 4(b). Twelve transducers were installed on the plate centerline which was directly above the propeller centerline. The transducer locations are shown in figure 4(b). The signals from the pressure transducers were recorded on magnetic tape and narrowband spectra were obtained for each of the test points. Typically the narrowband range was 0 to 10 000 Hz

with a bandwidth of 32 Hz. However, because the propeller blade passing frequency was so close to the wind tunnel compressor tone at some of the test conditions, some higher resolution narrowbands (0 to 2500 Hz with an 8 Hz bandwidth) were performed to isolate the propeller tone.

The data taken at varying tunnel Mach numbers with the propeller operated at an advance ratio of 3.06 were reduced to pressure-time histories using signal enhancement with a once-per-revolution signal as the trigger. This enhancement was necessary to obtain accurate time histories because of the high level of the tunnel background noise.

RESULTS AND DISCUSSION

Noise Variation with Swirl Recovery Vanes

Noise data were taken for the experimental test conditions listed in tables I and II. The noise data were taken at the same advance ratio for the SR-7A propeller model with the swirl recovery vanes at the forward and aft positions and with the propeller alone, without the swirl recovery vanes.

The addition of the swirl recovery vanes did not show any additional interaction noise within the range of transducer positions for any of the conditions tested. The interaction noise should theoretically peak at the far forward and far aft locations, particularly for this eight blade by eight vane configuration, and there may be some additional noise at these locations but none was observed for the existing range of transducer positions. Since the existing range of transducer positions covers the area of peak noise on the fuselage, any additional noise forward or aft of these locations is expected to have little impact on the cabin noise. Figure 5 shows the noise for the design condition, $M = 0.8$, $J = 3.25$, blade angle = 63.3° , vane angle = 86.1° , at the first three harmonics. These values were obtained from ordinary frequency domain spectra and the tone levels plotted were at least 6 dB above the broadband noise level. As can be observed, no additional noise appears to occur with the swirl recovery vanes at either the forward or aft positions. The far forward noise at the second and third harmonics is not shown since the tone was below the tunnel broadband level.

The noise around the peak noise location, near the propeller plane at 90 to 110° , is even slightly diminished with the addition of the swirl recovery vanes. The differences shown here are more than the typical data scatter. These trends can be seen even more clearly at some of the off-design conditions. For example figure 6 shows the data at $M = 0.75$, $J = 3.06$ for three propeller blade setting angles of 57.7 , 60.2 , and 63.3° . Looking first at 60.2° (fig. 6(b)) the noise without the vanes has the highest peak level. When the vanes are added at the aft position the noise is decreased and when the vanes are moved to the forward position the noise is decreased even further. This same pattern exists at the lower loading 57.7° blade setting angle but at the higher loading angle of 63.3° the noise is only reduced at the forward vane position.

These noise reductions appear to be reductions in the propeller loading noise as a result of the vane unloading the propeller. Figure 7 illustrates this unloading and is a plot of the propeller power coefficient C_p versus

advance ratio for the noise conditions of figure 6(b) ($M = 0.75$, and blade angle = 60.2°). As can be seen, the addition of the vanes lowers the power coefficient. The propeller alone has the highest C_p while the propeller with the vanes in the forward position has the lowest C_p . The highest C_p here in figure 7 corresponds to the most noise in figure 6(b) while the lowest C_p corresponds to the least noise. The noise variation also followed the trend of the loading variation for the 57.7 and 63.3° blade setting angles.

As can be seen in figure 7, the amount that the power coefficient is reduced is not large, the total being less than 4 percent. The noise reductions in figure 6(b) are larger than would be expected from a change in overall C_p of only 4 percent. It may be however, that the reductions in total C_p are from a larger percentage reduction at a localized section, perhaps at the tip, where most of the noise is being generated.

The data shown here indicate that the swirl recovery vanes were unloading the propeller and this resulted in lower propeller noise. Increases in interaction noise from the propeller wakes and vortices impacting the swirl recovery vanes were not observed for the range of transducer positions tested. The net result of this testing is that the addition of the swirl recovery vanes can provide a small peak noise reduction for the fuselage of an airplane at cruise conditions.

Noise Variation with Swirl Recovery Vane Blade Setting Angle

Some small peak noise variation was also observed with different swirl recovery vane blade setting angles. The experiments were performed with the vanes in the forward position and the propeller blade angle set at 63.3° . Three vane angles were tested; 84.7° , 86.1° , and 87.5° . Figure 8 shows the noise directivity at the design conditions of $M = 0.8$ and $J = 3.25$. The 86.1° blade setting angle showed the most recovered thrust of the three blade angles and the 84.7° angle showed the least recovered thrust. As can be seen in figure 8 the 86.1° vane angle showed the least noise while the 84.7° angle showed the most noise. This indicates that the better the vane performance the larger the peak noise reduction that might be achieved on the fuselage at cruise.

Propeller Alone Pressure-Time Histories

As observed before (ref. 1) the peak propeller blade passing tone first rises with increasing helical tip Mach number and then levels off or decreases at higher helical tip Mach numbers. This can be seen in figure 9 for the data taken in this experiment on the SR-7A propeller model. This propeller was operated at a constant advance ratio of 3.06 so each of the helical tip Mach number points was obtained at a different tunnel axial Mach number as indicated on figure 9. As can be observed, the data points were taken in steps of 0.02 axial Mach number from 0.7 to 0.86 to obtain a finer variation in helical tip Mach number than was obtained in the previous experiments.

In an attempt to understand what is happening at the higher helical tip Mach numbers, pressure-time histories were obtained for the transducer signals. These were obtained by signal enhancement using a once per revolution

signal from the propeller (synchronous time averaging). A typical pressure-time history is shown in figure 10. This was taken at the peak noise location at the $M = 0.72$, $M_{ht} = 1.03$ condition and represents an average of approximately 40 revolutions. The figure shows one pulse from each of the eight blades. The pulses consist of a broad positive portion and a sharp negative portion. This negative portion is larger than the positive portion and is a major contributor to the blade passing tone and its harmonics.

As the helical tip Mach number was increased to the peak noise value (fig. 9, $M = 0.8$, $M_{ht} = 1.15$), the pressure-time history of figure 11 was observed. This pressure time trace is very similar in shape to the one at $M = 0.72$, $M_{ht} = 1.03$, with a broad and slightly larger positive portion and a sharp negative portion. However, the negative portion of the pulse is showing the presence of a second positive pulse which is starting to fill in the negative portion. This is highlighted by the arrows in figure 11. The filling in of the negative portion of the pulse is starting to limit the growth of the blade passing tone with increasing helical tip Mach number.

As the helical tip Mach number was increased further, the second pulse became larger in strength and filled the negative pulse more completely. This can be seen in figure 12 which shows the pressure time-history at $M = 0.86$, $M_{ht} = 1.23$. Here the second pulse has partly filled the trough and is showing up as a second spike on the positive portion. It appears that this second pulse, with its cancelling interference on the first pulse, is the reason the peak noise does not continue to increase with helical tip Mach number. An understanding of the source of the second pulse is desirable.

During the propeller alone testing to obtain pressure-time waveforms, one of the eight propeller blades had a shortened chord at the tip. This was a result of some previous damage to the blade. Figure 13(a) shows a normal blade and figure 13(b) shows the trailing edge region of the shortened chord blade. The result of this shortened chord blade tip can be seen in the pressure-time history of figure 12. The last pulse on these traces is believed to be from the blade with the shortened tip chord. As can be seen from figure 12, the blade with the shortened tip chord has a smaller primary pressure-time signature than the other blades. This indicates, that at these conditions, the blade tip region is the controlling noise producing region of the blade. It can also be observed that the strength of the secondary pulse is reduced even more than the initial pulse indicating that the secondary pulse is from the same blade as the initial pulse.

One of the possible sources considered for the secondary pulse was a reflection of an initial blade pulse from some other surface, such as the tunnel walls, the propeller hub, or another propeller blade. An examination of the trace in figure 12 shows that the second pulse from the shortened blade is arriving behind the initial pulse by about one-fourth of the spacing between two blades. This one-fourth blade spacing distance would then have to be the difference in distance between the direct and reflected path lengths. In viewing the geometry, the noise path lengths to any of the possible reflecting surfaces are much larger than the distance between the primary and secondary pulses. The possibility of a direct reflection during the same revolution of the propeller is then eliminated. For the secondary pulse to be a reflection of the shortened blade's primary pulse, the reflection would then have to be arriving some whole number of revolutions of the propeller later than the

initial pulse and falling back onto the same initial blade pressure pulse. Although this scenario is theoretically possible for some specific propeller speed and transducer location, the timing of the reflected pulse would vary with a change in propeller speed or transducer position and the reflected pulse would fall someplace else in the pressure-time trace. The data at other propeller speeds and other transducer locations shows the same relative timing of the initial and secondary pulses. This then eliminates the possibility that the secondary pulse is a reflection of the initial pulse from the shortened blade.

Data from other sources also show the presence of this secondary pulse in the pressure-time history. Figure 14 is the pressure-time history of the SR-3 propeller model at the peak noise location, 107° , measured on the fuselage of the Jetstar airplane shown in figure 15. These experiments are described in reference 8. The propeller was operating at an axial Mach number of 0.805 and a helical tip Mach number of 1.14. These conditions were the highest reached during the airplane test and correspond roughly to the SR-7A conditions of figure 11. The pressure levels are lower here than for the SR-7A traces because the microphones are farther away and the airplane is at altitude with lower air density. As can be seen on figure 14, the secondary pulse is beginning to fill in the initial pulse just as it did for the SR-7A trace. The presence of this interfering pulse on a different propeller in a different type of test facility shows that this phenomena is not unique to the 8 by 6 wind tunnel or to the SR-7A propeller model.

The secondary pulse is then indicated as originating on the same propeller blade as the initial pulse. The spike type nature of the secondary pulse shape is similar to that for a shock wave and may be from a trailing edge shock on the blade. The secondary pulse could also be the result of the blade spanwise loading or thickness distribution. In any case, the secondary pulse is related directly to the blade and it may be possible to improve on this cancellation or shift it to another Mach number range if desired. To do this, however, will require a deeper understanding of the secondary pulse source.

CONCLUDING REMARKS

The SR-7A model propeller was tested for acoustics with and without downstream swirl recovery vanes. The swirl recovery vanes were installed in both forward and aft positions. The propeller wakes and vortices strike the downstream vanes and create an interaction noise source which is in addition to the propeller alone noise sources. The purpose of these experiments was to determine if this interaction noise had an effect on the total noise impacting the airplane fuselage at cruise.

The experiments with and without the swirl recovery vanes showed no additional noise from the installation of the vanes. The interaction noise occurs at the same frequency as the propeller alone blade passing tones and was not visible above the propeller alone tones at the transducer positions tested. It may be that the swirl recovery vane interaction noise contributes to the total noise at farther forward or farther aft positions but it should not significantly effect the cabin noise.

The presence of the swirl recovery vanes appears to unload the propeller. This lowers the loading noise generated by the propeller itself and results in small noise reductions. The reductions were observed near the propeller plane and corresponded to small reductions in the peak blade passing tone levels. The addition of the swirl recovery vanes was therefore observed to slightly lessen the airplane fuselage noise at the cruise condition.

The swirl recovery vanes were also tested at different blade setting angles while located in the forward position. Here the vane setting angle, which had the best performance in recovering the propeller swirl (most thrust addition), resulted in the least noise. This again demonstrated the slight noise advantage of the swirl recovery vanes.

The propeller alone noise variation with helical tip Mach number was also investigated during this experiment. As observed previously, the noise first rises with helical tip Mach number and then begins to level off or decrease at higher helical tip Mach numbers. In this experiment detailed pressure-time histories were taken at closely spaced helical tip Mach numbers. At the lower helical tip Mach numbers the primary pressure pulse from a blade has a broad positive portion and a sharp negative portion. In the region where the noise versus helical tip Mach number curve starts to level-off, a second pulse is observed. This second pulse starts to cancel the negative portion of the primary pulse and causes the noise to level-off. This second positive pulse appears to originate on the same blade as the primary pulse and is in some way connected to the blade itself. This leaves open the possibility of redesigning the blade to improve this cancellation.

REFERENCES

1. Dittmar, J.H.; and Stang, D.B.: Cruise Noise of the 2/9th Scale Model of the Large-Scale Advanced Propfan (LAP) Propeller, SR-7A. NASA TM-100175, 1987.
2. Dittmar, J.H.: Preliminary Measurement of the Noise from the 2/9 Scale Model of the Large-Scale Advanced Propfan (LAP) Propeller, SR-7A. NASA TM-87116, 1985.
3. Dittmar, J.H.; Jeracki, R.J.; and Blaha, B.J.: Tone Noise of Three Supersonic Helical Tip Speed Propellers in a Wind Tunnel. NASA TM-79167, 1979.
4. Dittmar, J.H.; and Jeracki, R.J.: Additional Noise Data on the SR-3 Propeller. NASA TM-81736, 1981.
5. Dittmar, J.H.; and Stang, D.B.: Noise Reduction for Model Counterrotation Propeller at Cruise by Reducing Aft-Propeller Diameter. NASA TM-88936, 1987.
6. Dittmar, J.H.: The Effect of Front-to-Rear Propeller Spacing on the Interaction Noise of a Model Counterrotation Propeller at Cruise Conditions. NASA TM-100121, 1987.

7. Dittmar, J.H.; Gordon, E.B.; and Jeracki, R.J.: The Effect of Front-to-Rear Propeller Spacing on the Interaction Noise at Cruise Conditions of a Model Counterrotation Propeller Having a Reduced Diameter Aft Propeller. NASA TM-101329, 1988.

8. Dittmar, J.H.: Further Comparison of Wind Tunnel and Airplane Acoustic Data for Advanced Design High Speed Propeller Models. NASA TM-86935, 1985.

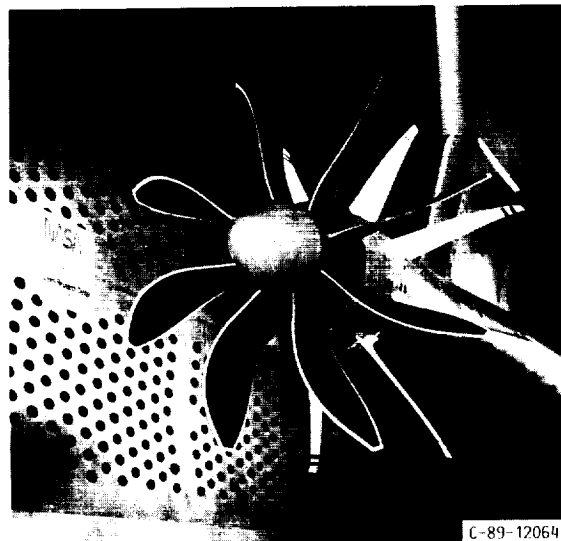
TABLE I. - SWIRL RECOVERY VANES AT 86.1° ANGLE WITH VANES OFF, VANES FORWARD, AND VANES AFT

Axial Mach number	Advance ratio at propeller blade angle, deg		
	57.7	60.2	63.3
0.8	----	----	4.0
	----	3.75	3.75
	3.5	3.5	3.5
	3.25	3.25	3.25
	3.06	3.06	----
0.75	2.9	----	----
	----	----	4.0
	----	3.75	3.75
	3.5	3.5	3.5
	3.25	3.25	3.25
0.7	3.06	3.06	3.06
	2.75	----	----
	----	----	4.0
	----	3.75	3.75
	3.5	3.5	3.5
0.65	3.25	3.25	3.25
	3.06	3.06	3.06
	2.75	----	----
	----	----	4.0
	----	3.75	3.75
0.6	3.5	3.5	3.5
	3.25	3.25	3.25
	3.06	3.06	3.06
	2.75	----	----
	----	----	4.0

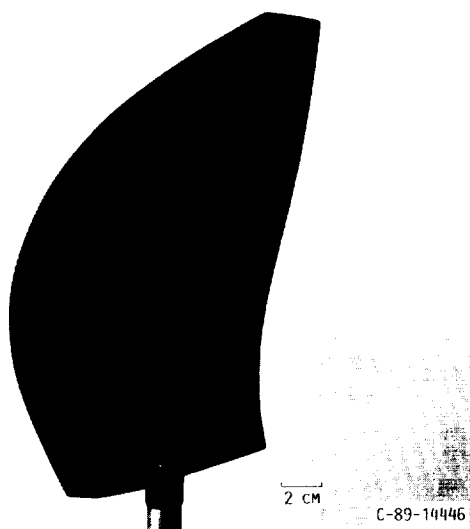
TABLE II. - PROPELLER AT 63.3° BLADE SETTING, ANGLE VANES IN FORWARD POSITION

Axial Mach number	Advance ratio at vane setting angles of 84.7, 86.1, and 87.5°
0.8	4.0
	3.75
	3.5
	3.25
0.75	4.0
	3.75
	3.5
	3.25
	3.06
0.7	4.0
	3.75
	3.5
	3.25
0.65	3.06
	4.0
	3.75
	3.5
0.6	3.06
	3.25
	3.5
	3.75

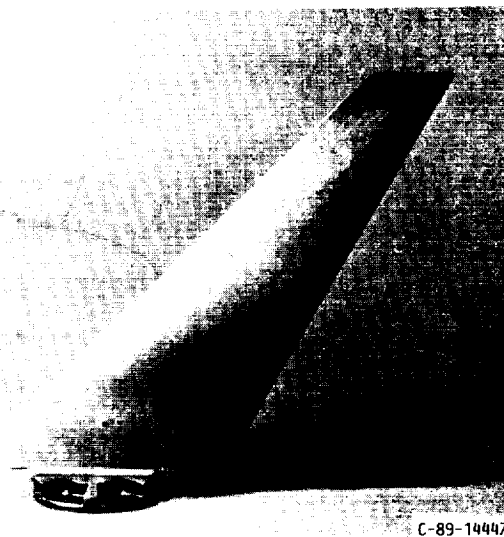
ORIGINAL PAGE
BLACK AND WHITE PHOTOGRAPH



(a) PROPELLER WITH SWIRL RECOVERY VANES.



(b) SR-7A PROPELLER BLADE.



(c) SWIRL RECOVERY VANE.

FIGURE 1. - SWIRL RECOVERY VANE APPARATUS.

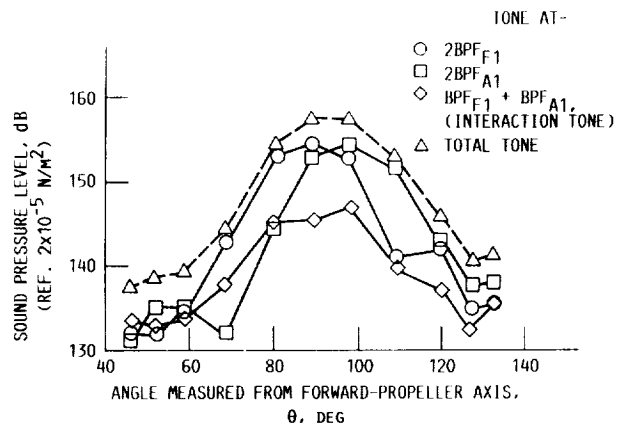
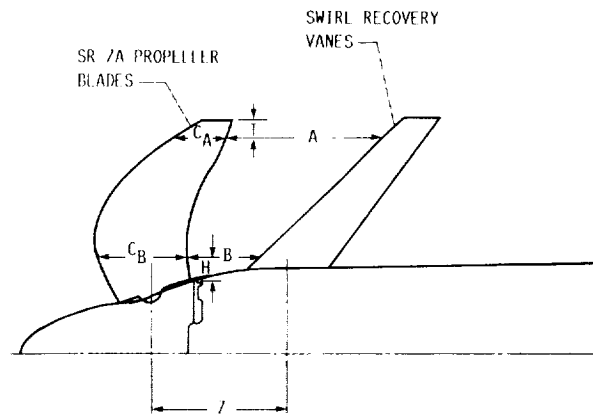


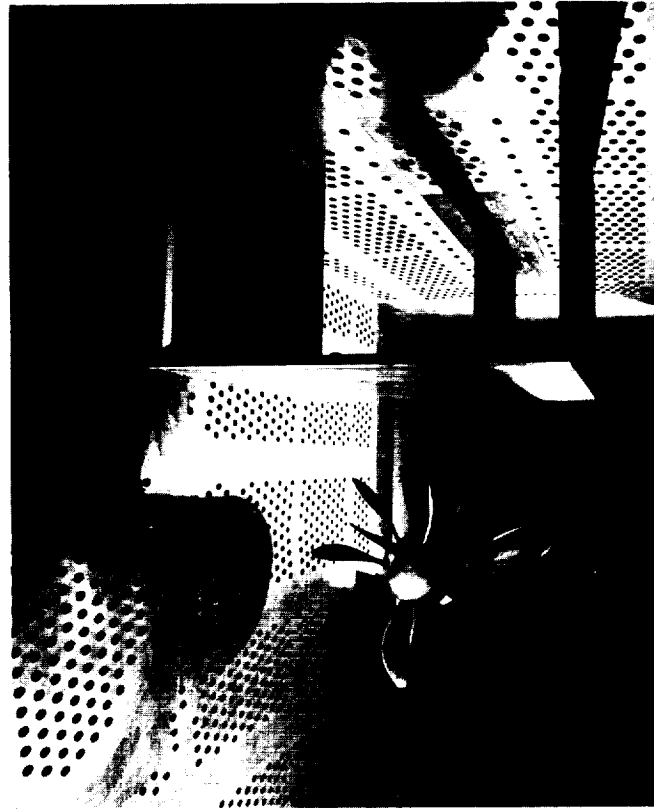
FIGURE 2. - SUMMATION OF TONES AT TWICE BLADE PASS-
ING FREQUENCY FOR COUNTERROTATION PROPELLER F1 - A1.



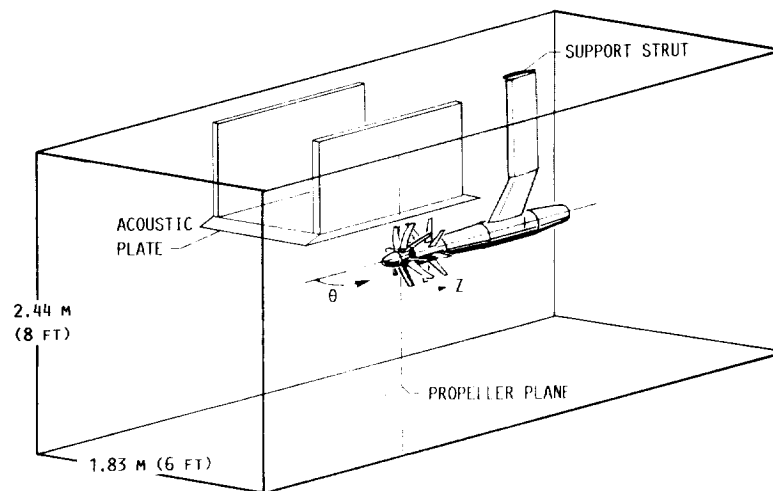
	SWIRL RECOVERY VANE POSITION, CM/IN.	
	FORWARD	AFT
A - DISTANCE FROM PROPELLER TRAILING EDGE TO VANE LEADING EDGE AT "T"	30.80 12 1/8	47.00 18 1/2
B - DISTANCE FROM PROPELLER TRAILING EDGE TO VANE LEADING EDGE AT "H"	15.24 6	31.44 12 3/8
C _A - PROJECTED CHORD OF PROPELLER BLADE AT "T"	3.65 1 7/16	3.65 1 7/16
C _B - PROJECTED CHORD OF PROPELLER BLADE AT "H"	12.07 4 3/4	12.07 4 3/4
H - DISTANCE OUT FROM HUB	4.45 1 3/4	4.45 1 3/4
I - DISTANCE IN FROM TIP	.95 3/8	.95 3/8
Z - DISTANCE FROM PROPELLER STACKING LINE TO VANE STACKING LINE	23.80 9.38	40.00 15 3/4

FIGURE 3. - SWIRL RECOVERY VANE POSITIONS.

BLACK AND WHITE PHOTOGRAPH



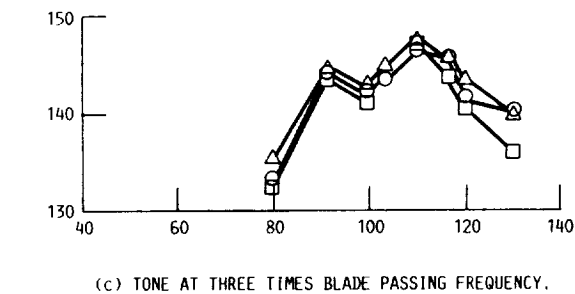
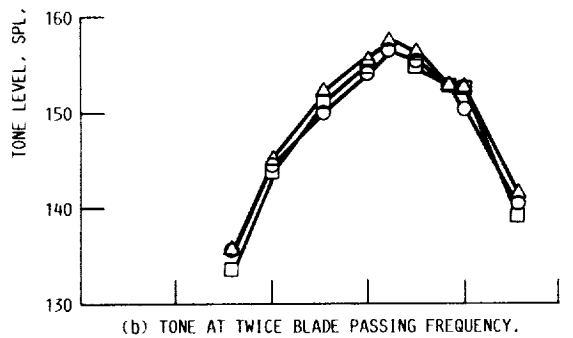
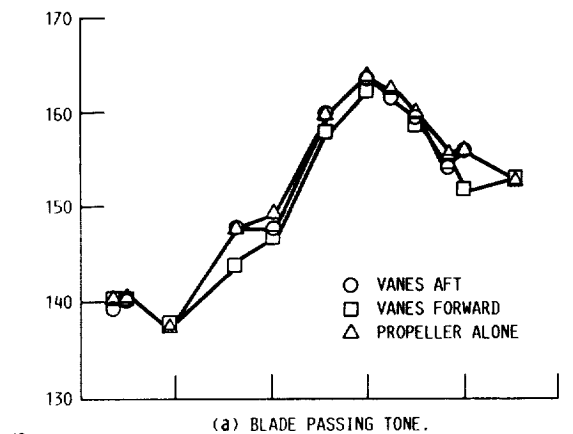
(A) PHOTOGRAPH.



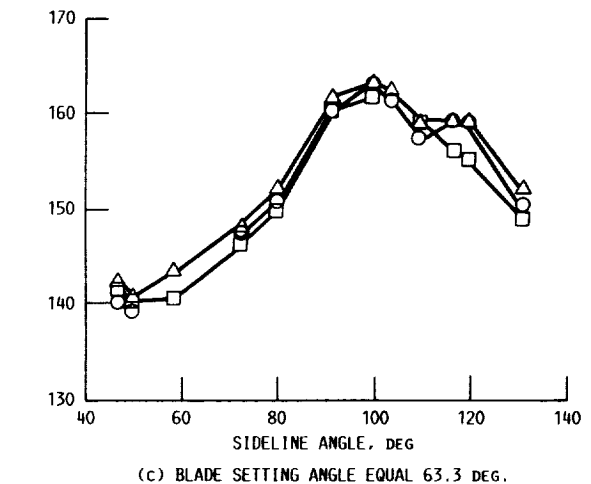
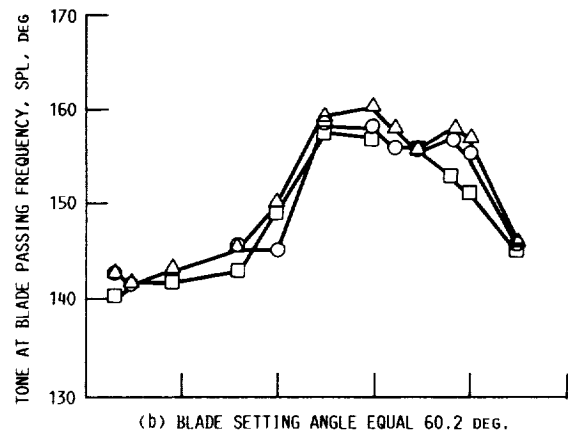
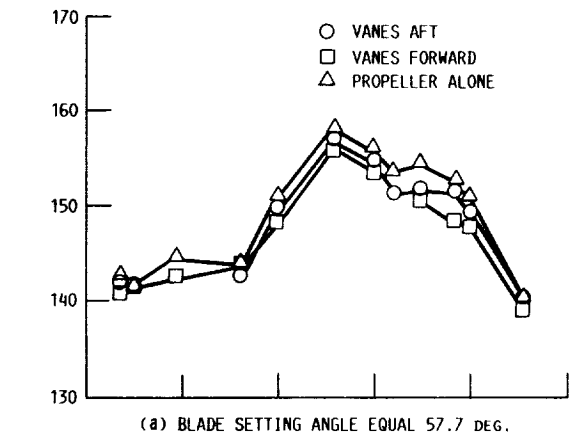
POSITION	TRANSDUCER (PLATE 0.3 DIAMETER FROM TIP)											
	1	2	3	4	5	6	7	8	9	10	11	12
	TRANSDUCER POSITION, CM (IN.)											
Z	-46.7 (-18.4)	-41.7 (-16.4)	-30.5 (-12.0)	-16.0 (-6.3)	-8.9 (-3.5)	0.8 (0.3)	8.9 (3.5)	12.4 (4.9)	18.0 (7.1)	25.0 (9.9)	28.7 (11.3)	42.4 (16.7)
	ANGLE FROM UPSTREAM, DEG											
θ	46.8	50.0	58.5	72.2	80	90.9	100	104	110	116.8	120	130.4

(B) TRANSDUCER LOCATIONS.

FIGURE 4. - ACOUSTIC PLATE.



(c) TONE AT THREE TIMES BLADE PASSING FREQUENCY.
FIGURE 5. - SWIRL RECOVERY VANE CRUISE NOISE DIRECTIVITY AT $M = 0.8$, $J = 3.25$, VANE SETTING ANGLE = 86.1° .



(c) BLADE SETTING ANGLE EQUAL 63.3° .
FIGURE 6. - SWIRL RECOVERY VANE CRUISE NOISE DIRECTIVITY AT $M = 0.75$, $J = 3.06$, VANE SETTING ANGLE = 86.1° .

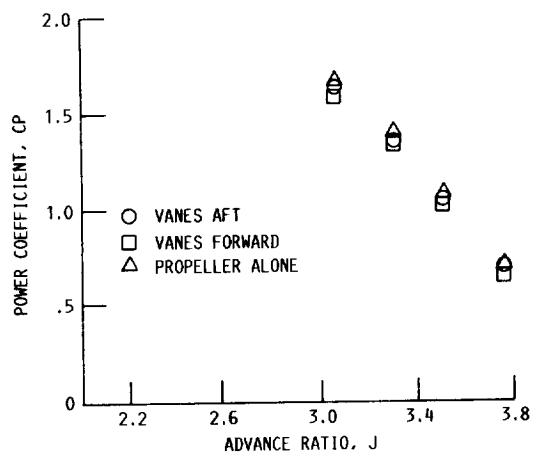


FIGURE 7. - POWER COEFFICIENT VARIATION WITH AND WITHOUT SWIRL RECOVERY VANES, $M = 0.75$, SR-7A BLADE SETTING ANGLE EQUAL 60.2° .

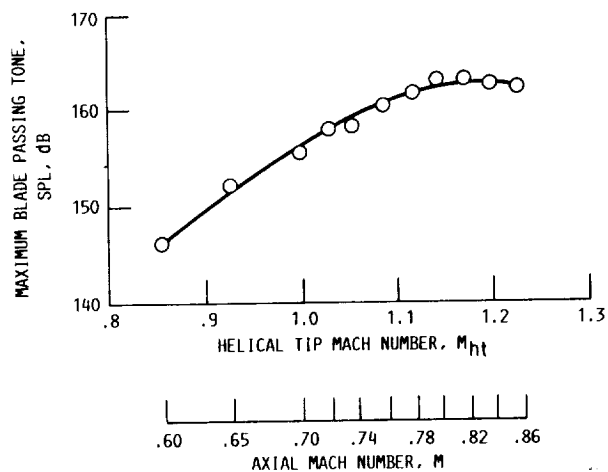


FIGURE 9. - MAXIMUM BLADE PASSING TONE VERSUS HELICAL TIP MACH NUMBER AT CONSTANT ADVANCE RATIO OF 3.06.

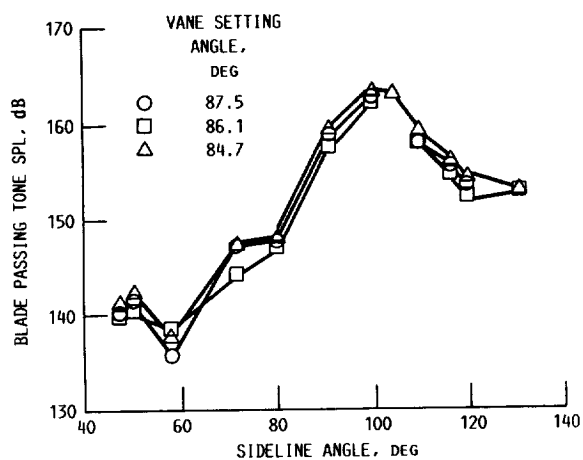


FIGURE 8. - CRUISE NOISE VARIATION WITH VANE SETTING ANGLE, $M = 0.8$, $J = 3.25$, BLADE SETTING ANGLE = 63.3° .

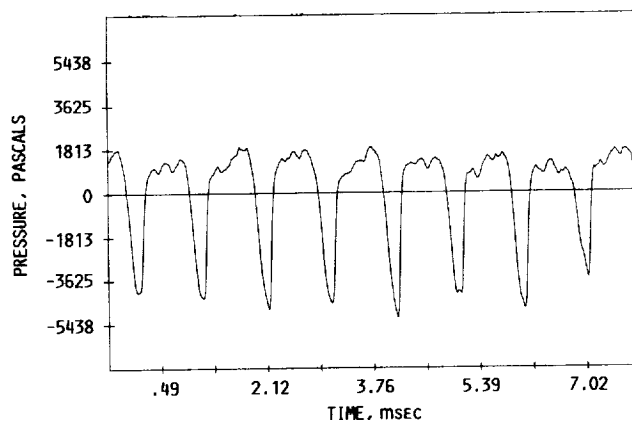


FIGURE 10. - PRESSURE-TIME HISTORY AT $M = 0.72$, $M_{ht} = 1.03$

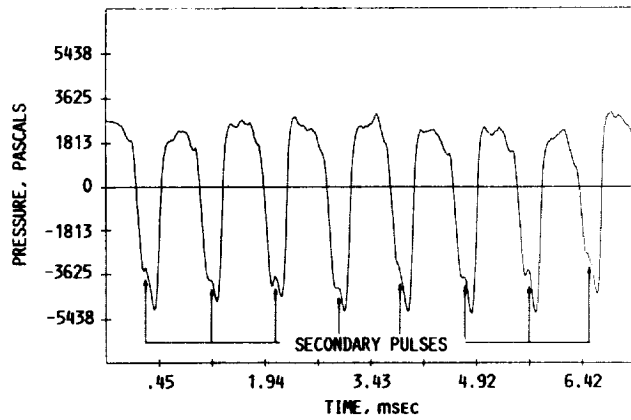
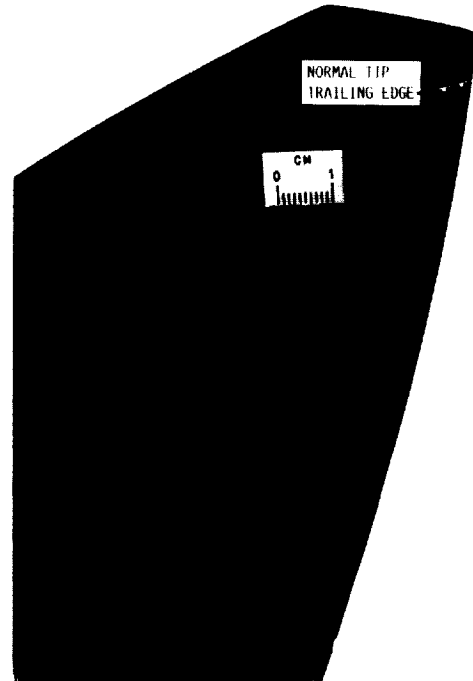


FIGURE 11. - PRESSURE-TIME HISTORY AT $M = 0.8$, $M_{ht} = 1.15$.



C-89-14449

(a) NORMAL BLADE TIP.

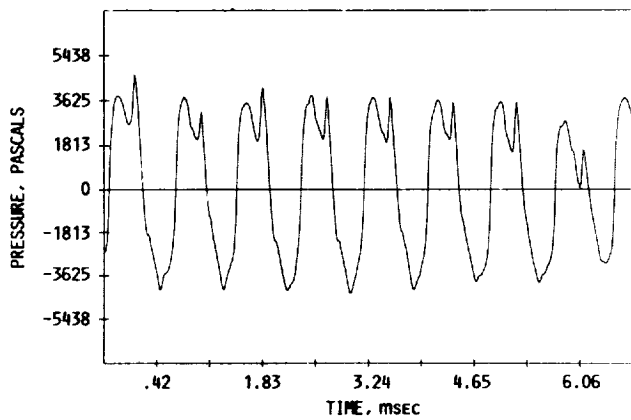
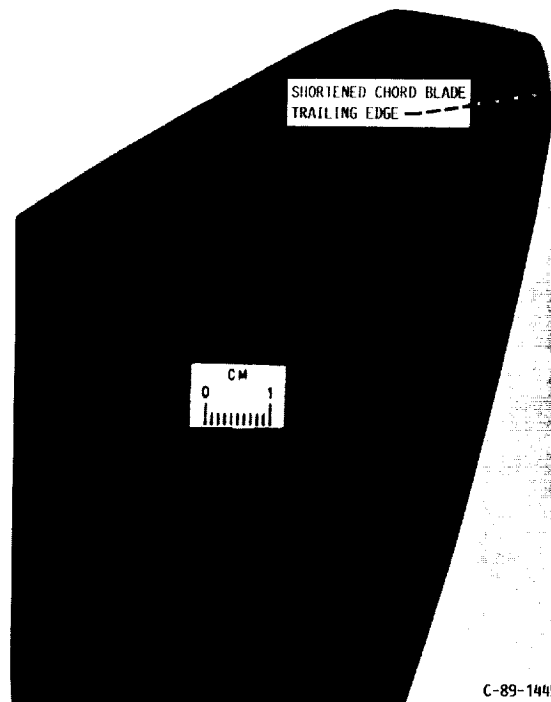


FIGURE 12. - PRESSURE-TIME HISTORY AT $M = 0.86$, $M_{ht} = 1.23$.



C-89-14450

(b) BLADE WITH SHORTENED TIP CHORD.

FIGURE 13. BLADE TIP SHAPE.

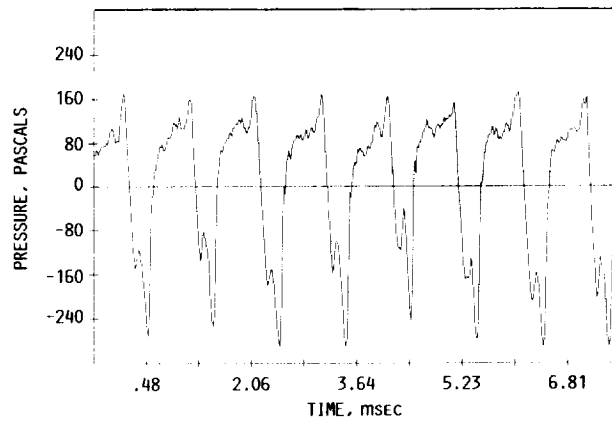


FIGURE 14. - PRESSURE-TIME HISTORY FROM SR-3 PROPELLER ON JETSTAR AIRPLANE.

CONVERT TO
BLACK AND WHITE PHOTOGRAPH



FIGURE 15. - SR-3 PROPELLER MODEL ON JETSTAR AIRPLANE.

Report Documentation Page

1. Report No. NASA TM-103625 AIAA-90-3932		2. Government Accession No.		3. Recipient's Catalog No.	
4. Title and Subtitle The Effect of Swirl Recovery Vanes on the Cruise Noise of an Advanced Propeller				5. Report Date	
				6. Performing Organization Code	
7. Author(s) James H. Dittmar and David G. Hall				8. Performing Organization Report No. E-5731	
				10. Work Unit No. 535-03-10	
9. Performing Organization Name and Address National Aeronautics and Space Administration Lewis Research Center Cleveland, Ohio 44135-3191				11. Contract or Grant No.	
				13. Type of Report and Period Covered Technical Memorandum	
12. Sponsoring Agency Name and Address National Aeronautics and Space Administration Washington, D.C. 20546-0001				14. Sponsoring Agency Code	
15. Supplementary Notes Prepared for the 13th Aeroacoustics Conference sponsored by the American Institute of Aeronautics and Astronautics, Tallahassee, Florida, October 22-24, 1990. James H. Dittmar, NASA Lewis Research Center; David G. Hall, Sverdrup Technology, Inc., Lewis Research Center Group, 2001 Aerospace Parkway, Brook Park, Ohio 44142.					
16. Abstract The SR-7A propeller was acoustically tested with and without downstream swirl recovery vanes to determine if any extra noise was caused by the interaction of the propeller wakes and vortices with these vanes. No additional noise was observed at the cruise condition over the angular range tested. The presence of the swirl recovery vanes did unload the propeller and some small peak noise reductions were observed from lower propeller loading noise. The propeller was also tested alone to investigate the behavior of the peak propeller noise with helical tip Mach number. As observed before on other propellers, the peak noise first rose with helical tip Mach number and then leveled off or decreased at higher helical tip Mach numbers. Detailed pressure-time histories indicate that a portion of the primary pressure pulse is progressively cancelled by a secondary pulse as the helical tip Mach number is increased. This cancellation appears to be responsible for the peak noise behavior at high helical tip Mach numbers.					
17. Key Words (Suggested by Author(s)) Propeller noise Noise Swirl recovery vane			18. Distribution Statement Unclassified - Unlimited Subject Category 71		
19. Security Classif. (of this report) Unclassified		20. Security Classif. (of this page) Unclassified		21. No. of pages 16	
				22. Price* A03	

National Aeronautics and
Space Administration

Lewis Research Center
Cleveland, Ohio 44135

Official Business
Penalty for Private Use \$300

FOURTH CLASS MAIL

ADDRESS CORRECTION REQUESTED



Postage and Fees Paid
National Aeronautics and
Space Administration
NASA 451

NASA
